Journals Pub

International Journal of
Energetic Materials

https://journalspub.com/journal/ijem/

ISSN: 2456-3978
Volume 11, Issue 1, 2025
January-June
DOI (Journal): 10.37628/IJEM

Research IJEM

Design and Implementation of a Prototype Micro Hydropower System Utilizing Jaffi Waterfalls, Nigeria

Ibrahim Salihu*

Abstract

Micro-hydroelectric power is a dependable and effective clean renewable energy source. Research presents Development of a prototype Experimental Hydro Electric power system using Jaffi waterfalls as a source of water supply. The objectives of the study are to design, construct, test and carry out performance evaluation of the prototype hydropower system using Jaffi waterfalls. The Prototype Hydropower system was designed and constructed using local readily available material that is relatively cheap. The performance evaluation test was carried out at the study site with a Net head of 10 m and variable flow rate ranging from 0.0001–0.0004 m^3/s. The experimental results show that two control valves opening has minimum and maximum values of output power of 14.64 and 28.95 W and a corresponding voltage of 12.20 and 16.45 V, respectively. While experimental results with one control valve opening (one Jet) have minimum and maximum output power of 19.21 and 44.08 W and a corresponding voltage of 15.25 and 21.50 V, respectively. The results of the two experiments show that a prototype system with one control valves opening higher which is enough to light LED energy saving bulbs and charging of small battery bank.

Keywords: Development, design, energy, hydro-electric, power system, prototype, waterfalls

INTRODUCTION

Energy is one of the most important aspects of world progress. It powers vehicles, televisions, musicals, and other household appliances in addition to running machinery and illuminating towns and houses. Human survival in the cosmos depends on energy, which is also crucial for any nation's economic and technical progress [1]. Nigeria is largely affected by inadequate energy supply, as demand is a major predicament nowadays; hence, the current state of power has been the major problem of its underdevelopment [2]. With the expansion of both industries and the population, the demand for power is rising daily. Alternative means of electric power generation must be found considering the critical energy scenario. Energy-related issues like the oil crisis, climate change, the need for electricity, and limitations on whole-sale marketplaces have been more prevalent globally during the past ten years. Nonetheless, the underutilization of certain off-grid renewable energy generation opportunities has been connected to the sharp increase in energy demand above production levels [3]. The necessity for technological alternatives to ensure their resolution is indicated by the fact that these challenges are only getting worse. Using renewable energy sources that do not harm the environment, such wind, solar, tidal, and hydroelectric power plants, to generate electricity closer to the consumption location is one of these technological options [4]. The present available hydropower system is not adequate and is also not accessible to all consumers. Biomass and fossil fuel-based energy are having serious health effects in the form of emissions and deforestation.

***Author for Correspondence**
Ibrahim Salihu
E-mail: ibrahimsalihu019@yahoo.com

Research Scholar, Department of Physics, College of Education Waka-Biu, P.M.B 1502 Waka - Biu Borno State, Nigeria.

Received Date: December 18, 2024
Accepted Date: January 08, 2025
Published Date: February 03, 2025

Citation: Ibrahim Salihu. Design and Implementation of a Prototype Micro Hydropower System Utilizing Jaffi Waterfalls, Nigeria. International Journal of Energetic Materials [IJEM]. 2025; 11(1): 1–12p.

These are also very expensive and not readily available to rural communities. Literature-based investigations reveal that hydropower potentials in Nigeria are huge, and these typical sources of energy are not being utilized effectively for power generation. This research work will highlight the potential for electricity based on the use of Jaffi waterfalls located in the Kwaya-Kusar Local Government Area of Borno State, Nigeria. The system is expected to provide a clean and cheap source of energy for rural communities using micro hydroelectric facilities, as energy from fossil fuels currently in use is usually expensive and sometimes unaffordable. The hydropower plant is also expected to enhance the supply from the national grid. The objective of the research is to design and construct a prototype of the hydropower system for the Jaffi waterfalls, test, and carry out a performance evaluation of the prototype machine developed.

MATERIALS AND METHODS

With a population of 56.5 thousand according to the 2016 area census, Kwaya-kusar occupies an area of 732 km² and is primarily inhabited by Bura and Tera tribes. According to the United Nations Office for the Coordination of Humanitarian Affairs, most of the population of Kwaya-kusar is a subsistence farmer [5]. It demonstrates that most of the communities in the Kwaya-kusar area lack access to a sufficient supply of electric power, a problem for which our effort aims to provide a remedy. The Jaffi waterfall is in the Kwayakusar Area of Borno State, Nigeria, at latitude 10°30 11 N and longitude 11°50 36 E. It flows year-round and offers a peaceful, isolated setting that is perfect for excursions and other associated field trips. It descends from a plateau that is 15.4 meters high into a valley (Figures 1 and 2) [6].

Figure 1. Jaffi waterfalls during (a) dry season and (b) rainy season.

Figure 2. Jaffi waterfalls retreat upstream.

Materials Selection

The selection of materials must be carefully considered to design and build a successful prototype micro hydropower system. The materials must be safe, effective in preventing water from striking the turbine blades, structurally sound, and highly resistant to corrosion.

Lastly, the cost must be considered to ensure that the target audience can afford it.

Shaft

It is a kind of carbon steel that contains 0.05% to 0.25% carbon by weight. It is more machinable, welding-friendly, and malleable due to its reduced carbon content. Moreover, it has greater ductility and a broad range of applications. reasonably priced and cost-effective in comparison to steel equivalents. Therefore, it is recommended that this design work be done.

Casing

Common casing materials include steel, aluminum, wood, fiber sheets, and galvanized iron. These materials vary in price and weight, but they are quite durable and weather stable. Table 1 displays the characteristics of a few case materials. Steel is coated with zinc to create galvanized steel. Galvanized steel has a special set of qualities that make it highly resistant to corrosion, durable, recyclable, and formable. Because of its low density, low conductivity, and inexpensive cost, galvanized steel was selected for the casing.

Table 1. Properties of Casing Materials [7].

Material	**Thermal Conductivity (W/mK)**	**Density (kg/m^3)**	**Thickness (m)**
Fiber glass sheet	0.048	2450	0.001–0.01
Galvanized steel	65	7833	0.001–0.003
Aluminum	228	2700	0.0005–0.007
Stainless steel	15.6	7913	0.0005–0.0036

Turbine

Strong, abrasive-resistant, and corrosion-resistant materials ought to be used for the turbine blades. Particular attention is paid to maintaining extremely low material costs for the turbine runner's production [8]. Various materials used for turbine runners and their properties are presented in the Table below, such as stainless steel, cast iron and aluminum alloy.

Stainless steel has the properties of corrosion resistant, wear resistant and is most widely used in producing water turbine buckets. Grey cast iron is also used for turbine buckets because of its low cost and good machinability. Aluminum alloy is relatively cheap and readily available compared to stainless steel and grey cast iron.

Table 2. Parameters of Turbine Materials [9].

Properties	Stainless steel	Aluminum Alloy	Cast iron
Young Modulus (MPa)	1.90E5	7.27E4	1.253E5
Density (kg/m3)	7850	2700	7300
Tensile Yield Strength (MPa)	6.22E2	3.13E2-690	2.1E2
Tensile Ultimate Strength (MPa)	9.91E2	3.40E2	2.77E2
Hardness (MPa)	1.18E2 1.48E3	30–150	187
Fracture toughness (Mpam$^{1/2}$)	22–35	14–28	80–106
Poisson ratio	0.3	0.3	0.3

Penstock

Things to think about when choosing materials for a specific penstock design [10]. The necessary working pressure and diameter, the coupling method, weight, site accessibility, and ease of handling, Local pipe availability, projected lifespan and maintenance needs, kind of terrain to be traversed, and the impact of soil, climate, water quality, and potential tampering on the pipe.

Table 3. Properties of Penstock material [10–11].

	Mild Steel	**GFRP**	**HDPE**	**PVC**
Phase at STP	Solid	Solid	Solid	Solid
Young Modulus (GPa)	200	35–86	1.25	2.90–3.30
Density (kg/m^3)	7850	1250–2500	960	1380
Tensile Yield Strength (Mpa)	400–550	483–4580		50–80
Melting point (°C)	1450	1135	120–180	212
Thermal conductivity (w/mk)	44–52	0.18		0.16
Linear expansion (–°C)	9.9X10^{-6}	(6.0–10) E-6	12E15	8X10^{-5}
Water absorption (%)	–	–	0.02	0.04–0.4
Elongation at break (%)	15	(1.2–5.0)	15%	20–40

Turgo Turbine Design Calculation/ Analysis

The pressure at the bottom of the penstock creates a jet of water with velocity, (v_{jet})

$$v_{jet} = k_n\sqrt{2gH_n} \tag{1}$$

k_n = Nozzle velocity coefficient (normally ranges from 0.95–0.99). For this case $k_n = 0.98$

Flow rate (Q) is then given by the velocity above multiplied by the cross-sectional area of the site.

$$Q = A_{jet} \times v_{jet} \times n_{jet} \tag{2}$$

$$Q = \frac{d^2{}_{jet}}{4} \times v_{jet} \times n_{jet}$$

where:
n_{jet} is the number of jets and d_{jet} is the diameter of the jet (m)

solving ford_{jet}.

$$d = \frac{0.54}{H^{\frac{1}{4}}_n} \times \sqrt{\frac{Q}{n_{jet}}} \tag{3}$$

Design Analysis for the Number of Buckets

Number of Buckets, Z is given by the equation below

$$z = 15 + \frac{PCD}{2d} \tag{4}$$

Based on research carried out by Yani et al. (2020) [12] on shapes of blades, spoon blades with a smaller number of blades tend to have higher electric efficiency. Also, Payambarpour et al. (2019) [13] reveals that increase in number of blades decrease in the flow through the turbine due to increase in turbine hydraulic resistance. For this present design, the number of buckets was reduced by 20%. There is a total number of buckets for this design, which stand at 16 buckets

Angle of sector of each bucket is given by:

$$\theta = \frac{pitch\ centre\ diametre}{number\ of\ blades} \tag{5}$$

Jet ratio, m is given by

$$m = \frac{PCD}{d_{jet}} \tag{6}$$

Absolute velocity, $U = x \times v_{jet}$ (7)

where: x = speed ratio which ranges from 0.45–0.50 and is used to produce the maximum power [14].

Turbine speed, N is given by

$$N = \frac{(60 \times v_{jet} \times x)}{(\pi \times PCD)} \tag{8}$$

The correlation between the specific speed (N_s) and the net head (H_n) is given by

$$N_s = 85.49 \times \sqrt{\frac{n_{jett}}{H_n^{0.243}}} \tag{9}$$

Velocity Triangle of a Turgo Turbine

Generally, the Turgo turbine efficiency is affected by several variables, such as the nozzle or the jet inclination angle, the speed ratio and the bucket design. In fact, the efficiency of the Turgo turbine for micro-projects is highly influenced by the jet inclined angle and the jet position [15]. The investigations carried out by [15–16] concluded that the highest efficiency of the studied Turgo turbine applied for low head micro-hydro plants was achieved for an optimal jet inclination angle of about 20°. Therefore, for this design, water strikes the blade at an angle of 20 degrees (Figure 3).

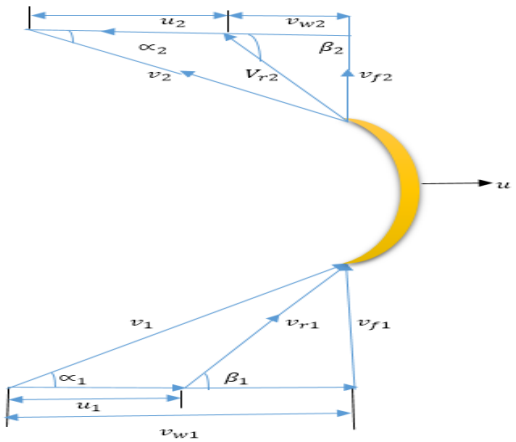

Figure 3. Velocity Diagram of a Turgor Turbine.

If the vane surface, loss of energy due to friction is zero

$$v_{r1} = v_{r2}$$
$$u_1 = u_2$$

where v_{rl} = Relative velocity of the jet and vane at the inlet, v_{r2} = Relative velocity of the jet and vane at the outlet, u_l = Velocity of the vane at the inlet, u_2 = Velocity of the vane at the outlet.

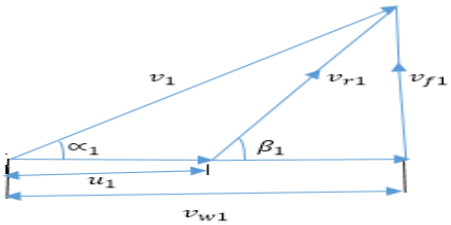

Figure 4. Inlet Velocity Diagram Triangle of a Turgor Turbine.

The velocity of the whirl at inlet of vane at inlet is giving by

$$v_{w1} = v_1 \times \cos \alpha_1$$

where v_1 = inlet velocity of the jet, α_1 = Angle between the direction of the jet and vane's direction of motion (Guide blade angle) (Figure 4).

The flow velocity at inlet is calculated as

$$v_{f1} = v_1 \times \sin \alpha_1 \tag{10}$$

$$\Longrightarrow v_{f1} = 16.6 \times \sin 20^{\circ} = 5.68 m/s$$

Angle between the relative velocity and vane's direction of motion (vane angle at inlet) is calculated as

$$\tan \beta_1 = \frac{v_{f1}}{v_{w1}} \tag{11}$$

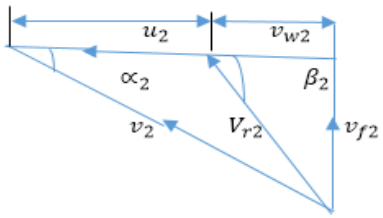

Figure 5. Outlet Velocity Diagram Triangle of a Turgor Turbine.

where v_2 = velocity of the jet at outlet, u_2 = Velocity of the vane at the outlet, v_{r2} = Relative velocity of the jet at outlet, v_{f2} = Velocity of flow at outlet, v_{w2} = Velocity of whirl at outlet, β_2 = Angle between the relative velocity and vane's direction of motion at outlet, α_2 = Angle between the direction of jet v_2 and vane's direction (Figure 5).

$$\cos \beta_2 = \frac{u_2}{v_{r2}} \tag{12}$$

$$v_2 = \sin \beta_2 \times v_{r2} \tag{13}$$

$$v_{w2} = v_{r2} - u_2 \tag{14}$$

$$v_{f2} = \sqrt{({v_2}^2 - {v_{w2}}^2)} \tag{15}$$

$$\alpha_2 = \tan^{-1}\left(\frac{v_{f2}}{v_{w2}}\right) \tag{16}$$

Mass of Water Striking the Vanes Per Second

Mass of water striking the vanes per second is in terms of relative inlet velocity between the jet and the blade and is given by

$$m = \rho_w a_j v_{r1} \tag{17}$$

where $m = mass\ flow\ rae\ of$ the water jet, $\rho_w =$ Density of water = 1000m^3/kg, $v_{rl} = Relative\ inlet\ velocity$, and a_j = velocity of the water jet at inlet

Force Exerted by the Jet of Water on Bucket.

Force exerted by the jet of water on bucket in the direction of motion of the blade is given by

$$F_x = \rho_w a_j v_{r1}[v_{w1} \pm v_{w2}] \tag{18}$$

$$\Rightarrow F_x = m[v_{w1} \pm v_{w2}]$$

But $\alpha_2 = 74^\circ$ which is less than 90°

$$\therefore F_x = m[v_{w1} + v_{w2}] \tag{19}$$

Work Done Per Second

Work done per second on the vane is given by

$$W.D/Sec = F_x \times u \tag{20}$$

Bucket Dimension of Turgo Turbine

The prototype modelof bucket and 3D Representation of the assembled Prototype Turbine Runner are shown in Figures 6 and 7, respectively.

The Width of the Bucket, w_b

The width of the bucket, w_b ranges from (1.68-2.34) d_j and is given by the relation

$$w_b = 2.2 \times d_j$$

$$\Longrightarrow w_b = 2.2 \times d_j = \tag{21}$$

Length of the Bucket l_b

The length of the bucket ranges from (2.4–3.4) d_j

$$\Longrightarrow l_b = 3.2 \times d_j = \tag{22}$$

Depth of the Bucket h_b

The depth of the bucket $h_b$is given by

$$h_b = 1.2 \times d_j \tag{23}$$

Figure 6. prototype Model of a Bucket.

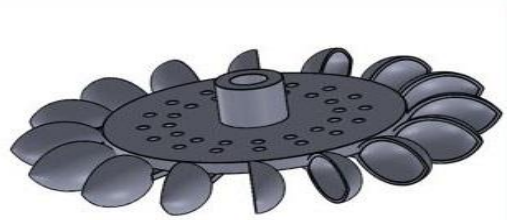

Figure 7. 3D Representation of the Assembled Prototype Turbine Runner.

Nozzle Design

The dimensions of the nozzle are determined according to the diameter of the jet (d_j)

- Nozzle diameter, $d_z = (1.151.25)\ times\ jet\ diameter$
- In this case $d_z = 1.18 \times d_j$
- Blocking space needle to nozzle tip, $n_p = 0.45 \times d_j$
- Location of the nozzle orifice radius $n_{or} = 0.503 \times d_j$
- Length of needle tip, $n_{tr} = 3.17 \times d_j$
- Curved of needle tip radius, $c_{tr} = 0.705 \times d_j$
- Curved of nozzle orifice radius, $n_{Cr} = 2.2 \times d_j$

Penstock Design Analysis

3D Representaion of the assembled prototype of Turgo Hydropower system and Orthographic view assembled prototype of Turgo Hydropower system are shown in Figures 9 and 10, respectively.

Internal Diameter of the Penstock

The diameter of internal penstock diameter D_P is calculated using the relation below

$$\Rightarrow D_p = 2.69 \times \left(0.009^2 \times 0.007^2 \times L_p/15.40\right)^{0.1875} \quad (24)$$

$$But\ length\ pipe\ L_p = \left(horizontal\ distance^2 + H_g{}^2\right)^{0.5}$$

The thickness of the penstock is calculated using equation () above

$$\Rightarrow t_p = \left(\frac{84+508}{400}\right) + 1.2(mm) \quad (25)$$

Safety Factor (SF)

This is the ratio of maximum stress or ultimate tensile strength to working stress. For penstock design a safety factor of less than 3 should not be recommended for any design penstock [10].
Mathematically SF is given as

$$s_f = \frac{(t_p \times s)}{(5\times10^3 \times H_g \times D_p)} \quad (26)$$

where S= Ultimate tensile stress of PVC = 28 x 10^6 N/m^2,

$\therefore$ *the penstock design is safe as calculated Safety Fcator is greater than 3*

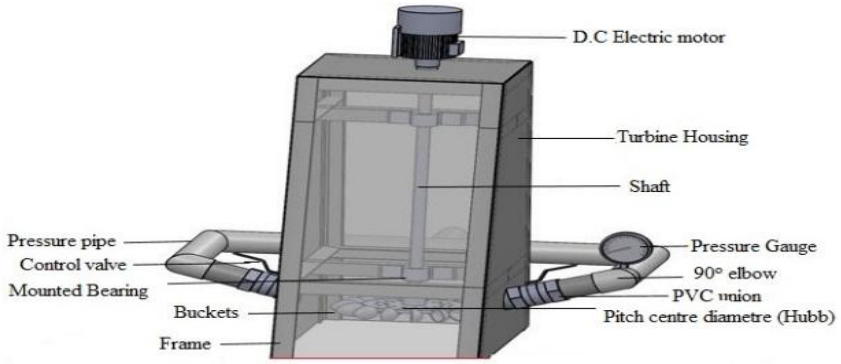

Figure 9. 3D Representaion of the Assembled Prototype of Turgo Hydropower System.

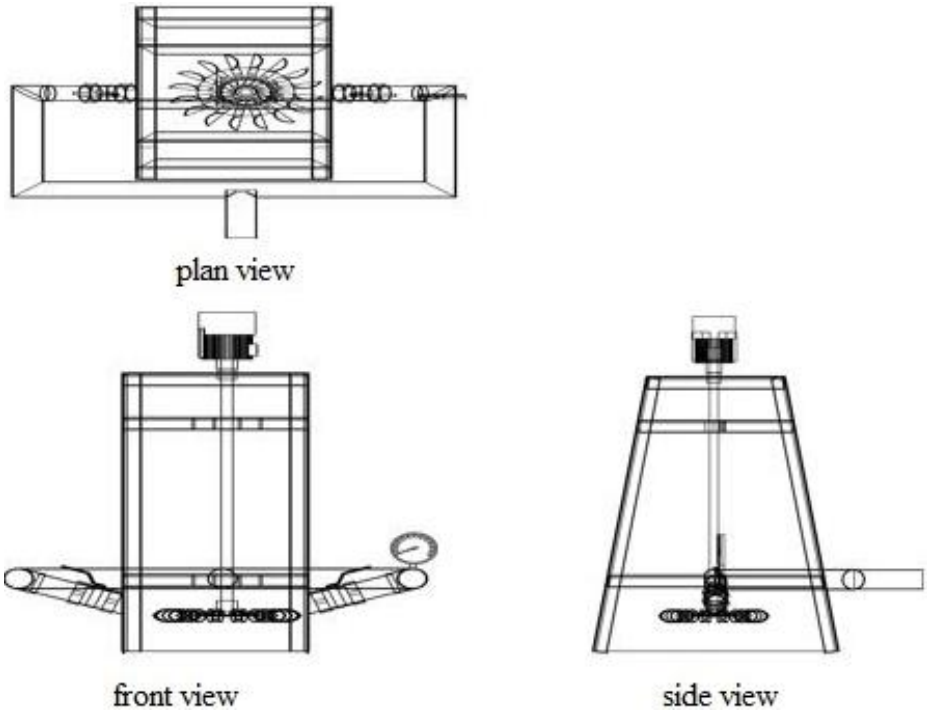

Figure 10. Orthographic View Assembled Prototype of Turgo Hydropower System.

RESULTS

Table 4. Experimental Results of Two Control Valves Opening at Constant Net Head of 10 m.

Flow-Rate, Q (m^3/s)	Shaft Rotational Speed, N (RPM)	Volt (v)	Curr. (A)	Power (w)	Eff. ε(%)
0.001	346.50	12.20	1.20	14.64	24.97
0.002	386.56	13.35	1.36	18.16	30.98
0.003	427.28	15.20	1.55	23.56	40.19
0.004	473.52	16.45	1.76	28.95	49.39

In the constructed prototype micro hydropower system test results using two control valves opening shown in Table 4, the turbine is capable to deliver a maximum power of 28.95W and an increase in the water flow, the shaft rotational speed also increases.

Table 5. Experimental Results of One Control Valves Opening at Constant Net Head of 10 m.

Flow-Rate, Q (m^3/s)	Shaft Rotational Speed, N (RPM)	Volt. (v)	Curr. (A)	Power (w)	Effi. ε(%)
0.001	462.50	15.25	1.26	19.21	32.77
0.002	486.32	17.50	1.46	25.55	43.59
0.003	670.58	19.36	1.68	32.52	55.48
0.004	712.53	21.50	2.05	44.08	75.20

In keeping the net head constant and varying the flowrate from 0.001 to 0.004m^3/s using one control valves opening as shown in Table 5 indicates that as the flow increases, the rotational speed increases to maximum speed of 712.53 rpm. The generator generates maximum potential difference of 21.50 V.

DISCUSSION

By opening the valve at the inlet of the two jets positioned at a 20° angle of attack, one can alter the water flow rate. The addition of valve openings in each variation results in an increase in water discharge, and the power increase is dependent on the shaft's rotational speed. The shaft's speed will increase as the valve is opened wider because the flow rate will be higher. Rotational torque has a significant impact on mechanical power. Though the mass of water entering the turbine will also have an impact on the momentum that occurs in the turbine blades, high rotation will often result in higher power.

Because torque, pressure, and losses are some of the variables that affect performance, Table 5 shows that high-power turbines do not always need to have two control valves operating on the turbine blades. Due to the notable rise in torque, there is a phenomena of power increase in the second test condition in every variation of water flow rate. As a result, the power has increased from the previous one.

Such conditions, where the turbine has a high rotation as well as high torque characteristics, are highly desirable. One control valve opened, resulting in a flow rate of 0.0004 m^3/s and a power of 44.08 W, while two control valves opened, resulting in two jets acting on the turbine blade, generating a power of 28.95 W at the same steady flow rate.

Based on the results obtained in Tables 4 and 5, it can be observed that the at constant net head and varying the flow-rate, the system efficiency has higher maximum efficiency attained at 0.004 m^3/s which corresponds to efficiency of 49.39% and 75.20% using two and one control valves opening, respectively.

The efficiency decreases as the turbine's rotational speed decreases. The rotation at each flow rate decreases as the torque derived from the direct coupling between the electric motor and the shaft increases. This indicates that the shaft will supply more energy because the turbine will need to carry more energy to rotate the electric motor when there is a greater torque. The turbine shaft has a reduced turn as a result of this circumstance. The turbine will be unable to rotate if the load is increased too high. in order for each turbine to receive the proper load based on the water's rotational power that can be transferred to the shaft for increased efficiency. When the load is converted to rotation, the same pattern will show up since a high rotation will result in a high torque. As the torque increases, the turbine shaft rotation decreases, so increasing the water discharge will likewise increase the turbine's power. When the load is converted to rotation, the same pattern will show up since a high rotation will result in a high torque. The turbine's output will rise in tandem with an increase in water outflow.

Though the mass of water entering the turbine will also have an impact on the momentum that occurs in the turbine blades, high rotation will often result in higher power. Turbine efficiency differs because of this. The turbine will be unable to rotate if the load is increased too high. so that each turbine receives the proper load according to the water's rotational power that can be transferred to the shaft.

CONCLUSIONS

In underdeveloped countries with erratic power sources, microgrids have been considered as a

potential way to make up for power shortages. Sometimes, certain operations, including charging phones, small devices, and low-energy lighting, require relatively little electricity. These needs can be met by creating, storing, and using micro-scale electricity when needed, rather than using fossil fuel generating plants that increase global emissions.The hydro turbine power system prototype was created and built utilizing readily available, reasonably priced components from the area. At a net head of 10 meters, a performance test was conducted in the field with an average flow discharge ranging from 0.0001/s to 0.0004 m^3/s, respectively. The developed prototype micro hydro-turbine power system performance evaluation was carried out using two control valves opening (two jets) and one control valve opening (one jet). The two experiments shows that a prototype system with one control valves opening has higher which is enough to light LED energy saving bulbs and charging of small battery bank

ACKNOWLEDGMENT

The Author gratefully acknowledges the financial support provided by the Tertiary Trust Fund (TET Fund) for sponsoring this research work. The funding enables me to explore innovative solutions and contribute meaningfully to the field.

Conflict of Interests

There is no conflict of interest.

REFERENCES

1. Oyedepo SO. Energy use and energy saving potentials in food processing and packaging: Case study of Nigerian industries. In Bottled and Packaged Water. Elsevier; 2019. pp.423–452.
2. Olatunji O, Akinlabi S, Oluseyi A, Abioye A, Ishola F, Peter M, et al. Electric power crisis in Nigeria: A strategic call for change of focus to renewable sources. 2018;413(1):012053.
3. Fakehinde OB, Fayomi OS, Efemwenkieki UK, Babaremu KO, Kolawole DO, Oyedepo SO.Viability of hydroelectricity in Nigeria and the future prospect. Energy Procedia. 2019;157: 871–878.
4. Fraenkel P, Paish O, Harvey A, Brown A, Edwards R, Bokalders V. Micro-hydro power. 1991.
5. Map of Kwaya-Kusar Local Government Area. 2022. Accessed online from https//reliefweb.int/sites/reliefweb.int/files/resources/1907217_nga_borno_kwaya_k usar_lga_map pdf.
6. Salihu I, El-Jummah AM, Oumarou MB. Feasibility study of Jaffi waterfalls as source of power generation for communities within and around Kwaya-Kusar locality, Borno, Nigeria. Cont J Eng Sci. 2019;14(1):1–14. https://doi.org/doi:10.5281/zendo.3253222.
7. Mahavar S, Sengar N, Rajawat P, Verma M, Dashora P. Design development and performance studies of a novel single family solar cooker. Renewable Energy. 2012;47:67–76.
8. Ebhota WS, Inambao FL. Smart design and development of a small hydropower system and exploitation of locally sourced material for pelton turbine bucket production. Iranian J Sci Technol. Trans Mech Eng, 2019;43(2):291–314.
9. Li J, Saw MMM. Design Optimization and Fatigue Analysis of Turgo Impulse Blade. 2018;154–157.
10. Obinna AC, Emmanuel OO, Chidozie O, Edward UM. Technical details for the design of a penstock for kuchigoro small hydro-power project. Am J Renew Sustain Energy. 2017;3(4):PP27–35.
11. Salleh M, Kamaruddin N, Mohamed-Kassim Z. Micro-hydrokinetic turbine potential for sustainable power generation in Malaysia. 2018;370(1):012053.
12. Yani A, Anoi R, Irianto J. Shape analysis of blade number for water prototype performance. J New Technol Res. 2020;6(4):PP46–53.
13. Payambarpour SA, Najafi AF, Magagnato F. Investigation of blade number effect on hydraulic performance of in-pipe hydro savonius turbine. Int J Rotating Mach. 2019.
14. Uniyal V, Kanojia N, Pandey K. Design of 5kw Pico Hydro Power Plant Using Turgo Turbine. Int J Sci Eng Res. 2016;7(12):363–367.

15. Cobb BR, Sharp KV. Impulse (Turgo and Pelton) turbine performance characteristics and their impact on pico-hydro installations. Renew Energy. 2013;50:959–964.
16. Gaiser K, Erickson P, Stroeve P, Delplanque JP. An experimental investigation of design parameters for pico-hydro Turgo turbines using a response surface methodology. Renew Energy. 2016; 85:406–418.

